Contribution from the Departments of Chemistry, University of South Carolina, Columbia, South Carolina 29208, and Columbia College, Columbia, South Carolina 29203

Molecular Distortions and Solid-State ^{113}Cd NMR: Crystal and Molecular Structure of the Piperidine Adduct of (5,10,15,20-Tetraphenylporphyrinato)cadmium(II), ^{113}Cd NMR Solution and Solid-State Spectra, and Potential Energy Calculations

P. F. Rodesiler,[†] E. A. H. Griffith,[‡] N. G. Charles,[‡] L. Lebioda,[‡] and E. L. Amma*[‡]

Received November 27, 1984

The crystal structure of the piperidine adduct of (5,10,15,20-tetraphenylporphyrinato)cadmium(II) *o*-xylene solvate has been determined. The structure is composed of isolated five-coordinate Cd(II) species with the *o*-xylene filling cavities between molecules. Only normal van der Waals distances are found between molecules. The Cd is displaced from the plane of the four pyrrole nitrogen atoms by 0.65 (2) Å with four Cd–N distances of 2.208 (3) Å and one axial Cd–N distance of 2.323 (3) Å. The local site symmetry of the Cd atom is C_1. The piperidine ring is in the chair conformation. There is some warping of the porphyrin skeleton. Potential energy calculations show that the location of the piperidine ring is in a minimum of ~30 kcal/mol. The chloroform solution ^{113}Cd NMR of a number of donor ligands with (5,10,15,20-tetraphenylporphyrinato)cadmium(II) has been measured and a chemical shift range of +418–498 ppm has been observed. For substituted pyridines a reasonable correlation of chemical shifts with base strength is shown. No such correlation seems to apply in general. The piperidine adduct gives a ^{113}Cd NMR signal in solution at 438 ppm deshielded. The corresponding solid-state MAS result is at 467 ppm, and the solid powder static spectrum shows an asymmetric signal corresponding to three components at 522, 467, and 412 ppm. This result is consistent with the geometry of the adduct from X-ray diffraction. Crystal data: triclinic, $P\bar{1}$, $Z = 2$, $a = 13.504$ (11) Å, $b = 14.753$ (5) Å, $c = 11.863$ (6) Å, $\alpha = 102.94$ (3)°, $\beta = 94.76$ (6)°, $\gamma = 91.04$ (5)°, $\rho_{obsd} = 1.31$ (2) g/cm^3, $\rho_{calcd} = 1.33$ g/cm^3, NO = 10672, NV = 556, $R_F = 0.053$, transmission factor range 0.834–0.800, $\mu = 5.15$ cm^{-1}, $\lambda = 0.71073$ Å, full-matrix refinement with anisotropic temperature factors and anomalous dispersion corrections.

Introduction

^{113}Cd NMR has been observed in a number of types of compounds ranging from simple inorganic salts through organometallic compounds to biological macromolecules.[1-3] It has shown considerable promise as a probe of metal ion sites in metalloenzymes, particularly the Zn sites in, e.g., alkaline phosphatase, carbonic anhydrase, carboxypeptidase, liver alcohol dehydrogenase, superoxide dismutase, metallothionein, and inorganic pyrophosphatase. It has also been utilized as a probe of the Ca^{2+} sites of calmodulin, parvalbumin, insulin, troponin C, and concanavalin A. The chemical shift range of Cd^{2+} of ~900 ppm lends itself to a possible utilization as a probe of the metal ion site during conformational changes in biological processes in which the metal atom environment undergoes changes. One such utilization would be to study the stress placed upon the metal site by the R ⇄ T allosteric transformation in hemoglobin. In principle, one should be able to observe the ^{113}Cd NMR in hybrid hemoglobins such as $\alpha_2Fe^{2+}\beta_2Cd^{2+}$, $\alpha_2FeCO\beta_2Cd^{2+}$, $\alpha_2Cd^{2+}\beta_2Fe^{2+}$, and $\alpha_2Cd^{2+}\beta_2FeCO$, where e.g. α_2Cd^{2+} represents the α chains in which the normally occurring iron is replaced by cadmium. From these observations one should be able to distinguish the different stresses placed upon the α, β metal sites by partial oxygenation or ligation. Toward this end we have made a number of derivatives of cadmium tetraphenylporphyrin and cadmium protoporphyrin IX (the naturally occurring porphyrin) and observed the ^{113}Cd NMR signal. We present here some of our results on the ligated cadmium porphyrins. Recent results by Ellis[4] and co-workers show that a number of factors are involved in the ^{113}Cd NMR chemical shift of cadmium porphyrins. Of particular interest here are the solution and solid-state ^{113}Cd NMR spectra and their relationship to the crystal structure and distortions of (tetraphenylporphyrinato)cadmium–piperidine.

Experimental Section

(5,10,15,20-Tetraphenylporphyrinato)cadmium(II) (CdTPP) was prepared by reacting cadmium acetate with *meso*-tetraphenylporphine in *N,N'*-dimethylformamide.[5] Typically, cadmium acetate was prepared by dissolving enriched (90% ^{113}Cd)CdO (52 mg, 0.40 mM; Oak Ridge National Laboratory) in an excess of glacial acetic acid (3 mL) and freeze-drying the solution to give $Cd(C_2H_3O_2)_2 \cdot H_2O$ (99% yield). *meso*-tetraphenylporphine (0.2452 g, 0.30 mM; Aldrich Chemical Co.) was added to the above in *N,N'*-dimethylformamide (45 mL). The reaction mixture was held at refluxing temperature (152 °C) with stirring for 15 min under a dry nitrogen atmosphere. The visible spectrum of the reaction mixture showed no bands due to unreacted *meso*-tetraphenylporphine. The reaction mixture was reduced to dryness in vacuo, and the residue was dissolved in benzene (30 mL); *n*-hexane (300 mL) was added, and the mixture was placed in a cold room (4 °C) overnight. CdTPP (0.2749 g, 95% yield) was isolated as a blue-black solid by filtration and vacuum-dried. The purity of this compound was inferred from the visible spectrum and ^{13}C and ^{113}Cd NMR.

Solvents and Ligands. Chloroform-*d* (99.8 atm % D, Gold Label) was obtained from Aldrich Chemical Co. and was used directly. Pyridine and piperidine were distilled from calcium hydroxide under a dry nitrogen atmosphere. Tetrahydrofuran and 1,4-dioxane were distilled from sodium–benzophenone ketyl. *N,N'*-Dimethylformamide was dried by using activated molecular sieves (4A) under a dry N_2 atmosphere. 1-Methylimidazole and 2-methylimidazole were obtained from Aldrich Chemical Co. Imidazole and triphenylphosphine were obtained from Columbia Organic Chemicals Co.

Preparation of CdTPP·L. Solid CdTTP was weighed and added to a graduated cylinder and chloroform-*d* added while the solution was stirred with a magnetic stirring bar. Ligands were added with a lambda pipet (Fisher Scientific Co.) or as a weighed solid.

Instruments. UV–visible spectra were obtained on a Beckman Model 35 UV–visible spectrometer using *N,N'*-dimethylformamide as a solvent. The ^{113}Cd FT spectra were obtained on a highly modified Varian XL-100-15 NMR spectrometer operating at 22.18 MHz, a Bruker WP-200 spectrometer, a Nicolet NC200 spectrometer, or a Bruker WH-400 spectrometer described elsewhere.[4,6] Chemical shift measurements were

[†] Columbia College.
[‡] University of South Carolina.

(1) Ellis, P. D. *Science* (*Washington, D.C.*) **1983**, *221*, 1141–1146 and references therein.
(2) Armitage, I. M.; Otvos, J. D. *Biol. Magn. Reson.* **1982**, *4*, 79–144.
(3) Rodesiler, P. F.; Turner, R. W.; Charles, N. G.; Griffith, E. A. H.; Amma, E. L. *Inorg. Chem.* **1984**, *23*, 999–1004 and references therein.
(4) Jakobsen, H. J.; Ellis, P. D.; Inners, R. R.; Jensen, C. F. *J. Am. Chem. Soc.* **1982**, *104*, 7442–7452. This paper contains much of the background material and relevant solid-state NMR references.
(5) Plese, C. F.; Amma, E. L.; Rodesiler, P. F. *Biochem. Biophys. Res. Commun.* **1977**, *77*, 837–844.
(6) Charles, N. G.; Griffith, E. A. H.; Rodesiler, P. F.; Amma, E. L. *Inorg. Chem.* **1983**, *22*, 2717–2723.
(7) Frenz, B. A. "Enraf-Nonius Structure Determination Package"; Enraf-Nonius: Delft, The Netherlands, 1982; Version 17 (with local modifications).
(8) (a) Stewart, J. M. "The X-RAY System", Tech. Rep. TR-445; Computer Science Center, University of Maryland: College Park, MD, 1979. (b) Ibers, J. A., Hamilton, W., Eds. "International Tables for X-ray Crystallography"; Kynoch Press: Birmingham, England, 1974; Vol. IV. (c) Due to software problems, the data set could not be accessed from X-RAY 79 and the refinement including hydrogen atoms was performed by the program SHELX on the VAX 11/780. Sheldrick, G. "Program for Crystal Structure Determination"; University of Cambridge, Cambridge, England: 1976.

0020-1669/85/1324-4595$01.50/0

Table I. Cell Data, Data Collection, and Refinement Parameters of $CdN_5C_{57}H_{49}$[a]

diffractometer: Enraf-Nonius CAD-4 interfaced to PDP 11/60
a = 13.504 (11) Å; b = 14.753 (5) Å; c = 11.863 (6) Å
α = 102.94 (3)°; β = 94.76 (6)°; γ = 91.04 (5)°
D_{measd} = 1.31 (2) g/cm^3; D_{calcd} = 1.33 g/cm^3
Z = 2; wavelength Mo Kα 0.71073 Å; V = 2294 (4) Å^3
fw = 916.41; space group $P\bar{1}$
μ = 5.15 cm^{-1}
size of cryst: 0.30 × 0.36 × 0.62 mm
faces: 10$\bar{1}$, $\bar{1}$01, 101, $\bar{1}$0$\bar{1}$, 110, $\bar{1}\bar{1}$0, 0$\bar{1}$1, 01$\bar{1}$, 001, 00$\bar{1}$, 100, $\bar{1}$00
abs cor made and transmission factor range[7] found were 0.870–0.834; graphite monochromator used, θ = 6.1°
P factor 0.030 in $\sigma(F_o^2) = [\sigma(I_{raw})^2 + (RI_{raw})^2]^{1/2}/Lp$ and $w = 1/\sigma(F_o)^2$
data considered non-zero if $F^2 > 4\sigma(F^2)$
13341 hkl's measd in ω–2θ mode to $2\theta_{max}$ = 60°; hkl range h = 0 to +18, k = −20 to +20, l = −16 to +16; 10672 reflcns used to solve and refine structure, 109 unobsd ($F_{min} > 13.0$)
variable scan speed with preliminary scan speed of 4°/min 2θ
25 general reflcns used in orientation matrix (checked every 24 h) and used for all parameter measmts
3 std reflcns monitored every 100 reflcns, decay less than 2% I
room temperature ~18 °C
structure refined by full-matrix least squares, including anisotropic temp factors and anomalous dispersion corrections with wts based upon intens statistics; function minimized here and below $\sum_i w_i[|F_{oi}| - |F_{ci}|]^2$[7]
final least-squares performed on Amdahl V6 with f, $\Delta f'$, and $\Delta f''$[8a] from ref 5b
largest shift at end of refinement 0.03σ, av < 0.001σ
no. of variables 556; final R = 0.053, weighted R = 0.048[8c]
$F(000)$ = 948
final difference Fourier qualitatively featureless

[a] Solvent molecules treated as rigid groups.

Table II. ^{113}Cd NMR Results of CdTPP·L in Chloroform-d Solution[a]

L	chem shift, ppm[b]	pK_a	σ,[e] ppm
	CdTPP·L		
pyridine	425 (2)	5.25	...
4-picoline	423 (2)	6.02	−0.17
4-acetylpyridine	432 (2)	...	+0.66
4-aminopyridine	418 (2)	9.11	−0.66
3-chloropyridine	432 (2)	2.84	+0.37
piperidine	438 (2), 468 (-)[f]	11.1	...
imidazole	491 (2)	6.95	
1-methylimidazole	421 (2)	7.33	
1,2-dimethylimidazole	429 (2)	...	
2-methylimidazole	no resonance obsd		
tetrahydrofuran	434 (2)		
triphenylphosphine	498 (2)		
	CdTPP·L$_2$		
p-dioxane	435 (2)		
tetrahydrofuran	425 (2)		
	CdTPP (35 °C)		
	476 (1)[c]		

[a] Concentration-independent results. [b] Positive values are deshielded relative to 0.1 M $Cd(ClO_4)_2$ in H_2O standard. [c] This is presumably the four-coordinate Cd(II) species. [d] Half-width at half peak height. [e] Hammet σ constant. [f] Solid-state MAS (centroid).[3]

made with respect to an external standard of 1.0 M $CdCl_2$ in a 50/50 mixture by volume of H_2O/D_2O or 0.1 M $Cd(ClO_4)_2$ in a 50/50 mixture by volume of H_2O/D_2O. All chemical shifts are reported relative to 0.1 M $Cd(ClO_4)_2$. Positive chemical shifts are deshielded relative to the standard. Diffraction-quality crystals of CdTPP·pip (pip = piperidine) were grown by adding piperidine and o-xylene to a CdTPP·diox (diox = dioxane) solution and placing the sealed flask under nitrogen in a refrigerator. High-quality crystals grew over a period of several weeks. Crystals were placed in thin-walled capillaries, diffraction data were collected, and the structure was solved and refined as indicated in Table I. Table III contains the atomic coordinates and B_{eq} values. Table IV contains the bond distances and angles. The F_o, F_c tables and anisotropic thermal parameters have been deposited as supplementary material.

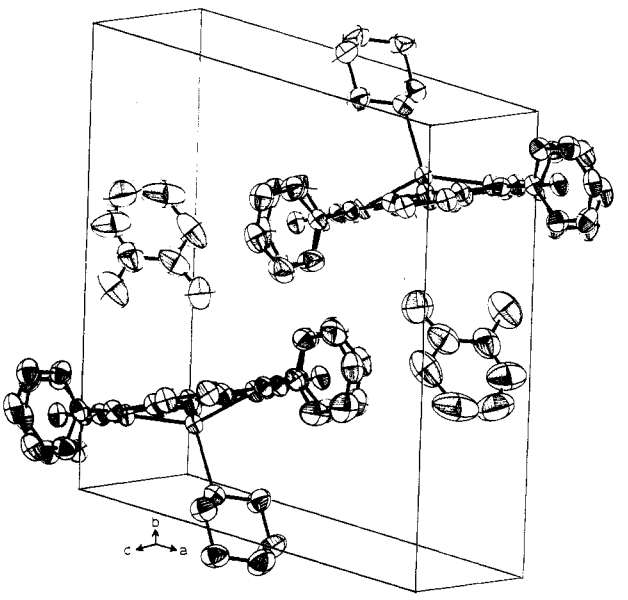

Figure 1. ORTEP view of the contents of the unit cell of the piperidine adduct of (5,10,15,20-tetraphenylporphyinato)cadmium(II) o-xylene solvate. The origin of the unit cell is in the lower rear left hand corner with axes as indicated.

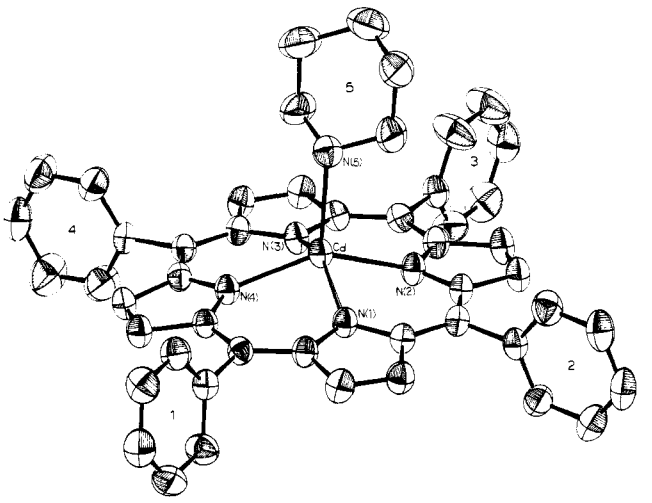

Figure 2. ORTEP view of an isolated molecule of the piperidine adduct of (5,10,15,20-tetraphenylporphyrinato)cadmium(II). The ellipsoids are drawn at the 50% probability level. It is clear from the figure that the piperidine molecule is in the chair conformation. For clarity, not all the atom notation is included in the figure. The notation used in the tables is consistent with the figures and is built around the following logistics: The α-carbon atoms are numbered from the left on N(1) as C(1A) to the right on N(1) as C(2A) and then around the pyrrole nitrogens in a systematic counterclockwise rotation, C(3A)...C(8A). The β-carbon atoms are labeled such that C(1B) is bound to C(1A), C(2B) bound to C(2A) and C(1B), and systematically counterclockwise around to C(8B) bound to C(8A). The M carbon atoms are denoted as C(M1) is bound to C(1P1) of phenyl ring 1, C(M2) is bound to phenyl ring 2 via C(1P2), etc. The notation of the phenyl rings is denoted for ring 1 by C(1P1)...C(6P1) in a counterclockwise position, for ring 2 by C(1P1)...C(6P2) in a clockwise fashion, for ring 3 by C(1P3)...C(6P3) in a counterclockwise fashion, and for ring 4 by C(2P4)...C(6P4) in a clockwise mode; the piperidine ring notation is denoted by C(2P5) bound to the right of N(5) and goes around to C(6P5) counterclockwise.

Results

Table II summarizes the solution, MAS, and static powder solid-state ^{113}Cd NMR results. Table III contains the atomic positional parameters with equivalent isotropic temperature factors, and Table IV contains interatomic distances and angles with

Table III. Fractional Atomic Coordinates with Esd's in Parentheses and Equivalent Isotropic Temperature Factors

	x/a	*y/b*	*z/c*	*B*, Å^2		*x/a*	*y/b*	*z/c*	*B*, Å^2
Cd(2+)	0.2256 (0)	0.1886 (0)	0.2602 (0)	2.95	C(1P2)	−0.1049 (3)	0.1758 (3)	0.0249 (3)	3.13
N(1)	0.1760 (2)	0.1691 (2)	0.0756 (2)	3.02	C(2P2)	−0.1599 (3)	0.0917 (3)	0.0041 (4)	4.28
N(2)	0.0780 (2)	0.2492 (2)	0.2898 (3)	3.26	C(3P2)	−0.2516 (3)	0.0835 (3)	−0.0621 (4)	4.77
N(3)	0.2781 (2)	0.2918 (2)	0.4205 (3)	3.07	C(4P2)	−0.2871 (3)	0.1553 (4)	−0.1084 (4)	4.60
N(4)	0.3742 (2)	0.2092 (2)	0.2058 (2)	2.92	C(5P2)	−0.2327 (3)	0.2372 (4)	−0.0872 (4)	4.75
N(5)	0.2125 (2)	0.0546 (2)	0.3308 (3)	3.66	C(6P2)	−0.1412 (3)	0.2503 (3)	−0.0193 (4)	3.90
C(1A)	0.2347 (3)	0.1469 (3)	−0.0148 (3)	3.04	C(1P3)	0.0648 (3)	0.3651 (3)	0.6064 (3)	3.15
C(1B)	0.1705 (3)	0.1246 (3)	−0.1228 (3)	3.64	C(2P3)	0.0361 (4)	0.3077 (3)	0.6752 (4)	5.51
C(2A)	0.0782 (3)	0.1644 (3)	0.0304 (3)	3.05	C(3P3)	−0.0118 (4)	0.3455 (4)	0.7723 (5)	7.08
C(2B)	0.0756 (3)	0.1352 (3)	−0.0947 (3)	3.62	C(4P3)	−0.0307 (4)	0.4392 (4)	0.8021 (4)	5.55
C(3A)	−0.0044 (3)	0.2269 (3)	0.2130 (3)	3.15	C(5P3)	−0.0015 (4)	0.4936 (3)	0.7336 (4)	5.15
C(3B)	−0.0910 (3)	0.2536 (3)	0.2765 (4)	3.86	C(6P3)	0.0479 (3)	0.4593 (3)	0.6337 (4)	4.33
C(4A)	0.0495 (3)	0.2890 (3)	0.3969 (3)	3.23	C(1P4)	0.5590 (3)	0.3187 (3)	0.4623 (3)	3.02
C(4B)	−0.0583 (3)	0.2914 (3)	0.3888 (4)	3.84	C(2P4)	0.5985 (3)	0.4050 (3)	0.4616 (5)	5.46
C(5A)	0.2192 (3)	0.3251 (3)	0.5079 (3)	3.01	C(3P4)	0.6897 (4)	0.4339 (4)	0.5252 (5)	6.62
C(5B)	0.2833 (3)	0.3646 (3)	0.6116 (3)	3.58	C(4P4)	0.7405 (3)	0.3782 (4)	0.5846 (4)	5.19
C(6A)	0.3752 (3)	0.3086 (3)	0.4620 (3)	2.97	C(5P4)	0.7013 (4)	0.2931 (4)	0.5826 (5)	5.89
C(6B)	0.3789 (3)	0.3553 (3)	0.5840 (3)	3.52	C(6P4)	0.6092 (3)	0.2600 (3)	0.5211 (4)	4.80
C(7A)	0.4575 (3)	0.2440 (3)	0.2796 (3)	2.93	C(2P5)	0.1077 (3)	0.0256 (3)	0.3358 (4)	5.13
C(7B)	0.5433 (3)	0.2345 (3)	0.2128 (3)	3.47	C(3P5)	0.0972 (4)	−0.0621 (4)	0.3790 (4)	5.83
C(8A)	0.4034 (3)	0.1810 (3)	0.0968 (3)	2.86	C(4P5)	0.1543 (5)	−0.0544 (4)	0.4945 (5)	6.58
C(8B)	0.5100 (3)	0.1965 (3)	0.1006 (3)	3.47	C(5P5)	0.2604 (4)	−0.0246 (4)	0.4910 (5)	7.14
C(M1)	0.3397 (3)	0.1492 (3)	−0.0051 (3)	2.91	C(6P5)	0.2677 (3)	0.0617 (4)	0.4445 (4)	5.42
C(M2)	−0.0054 (3)	0.1878 (3)	0.0946 (3)	3.05	C(6)	0.3081 (4)	0.5234 (3)	−0.0328 (4)	8.27
C(M3)	0.1144 (3)	0.3239 (3)	0.4981 (3)	3.08	C(1)	0.2318 (4)	0.4553 (3)	−0.0515 (4)	8.75
C(M4)	0.4588 (3)	0.2873 (3)	0.3975 (3)	2.88	C(5)	0.2211 (4)	0.4016 (3)	0.0301 (4)	11.65
C(1P1)	0.3888 (3)	0.1214 (3)	−0.1165 (3)	3.01	C(4)	0.2866 (4)	0.4162 (3)	0.1303 (4)	15.96
C(2P1)	0.3921 (3)	0.1812 (3)	−0.1919 (4)	4.06	C(3)	0.3629 (4)	0.4843 (3)	0.1489 (4)	16.80
C(3P1)	0.4402 (4)	0.1548 (4)	−0.2920 (4)	4.83	C(2)	0.3736 (4)	0.5379 (3)	0.0674 (4)	8.30
C(4P1)	0.4836 (3)	0.0683 (3)	−0.3198 (4)	4.32	C(7)	0.3232 (6)	0.5747 (5)	−0.1192 (6)	10.82
C(5P1)	0.4790 (3)	0.0105 (3)	−0.2465 (4)	4.39	C(8)	0.4515 (5)	0.6109 (5)	0.0930 (7)	10.85
C(6P1)	0.4316 (3)	0.0340 (3)	−0.1427 (4)	4.01					

derived quantities for CdTPP·pip. ORTEP[9] drawings of the isolated molecule and molecular packing are shown in Figures 1 and 2, respectively.

Discussion of Results

The structure may be described as made up of isolated CdTTP·pip molecules and *o*-xylene molecules of solvation (Figure 1) separated by ordinary van der Waals distances. The *o*-xylene molecules fill cavities formed by packing of the five-coordinate metalloporphyrin. The CdTPP·pip molecules may be most simply described as a typical five-coordinate M(II) metalloporphyrin complex[10] (Figure 2), in which the metal is displaced from the plane of the four pyrrole nitrogen atoms (a plane with displacements less than 0.01 Å) by 0.65 Å toward the axial ligand, the M–Ct distance notation of Scheidt.[10] The Cd–N(pyrrole) distances average 2.203 Å with a spread of ±0.032 Å and individual errors of ±0.003 Å and are comparable to those found in CdTPP·2diox,[11] 2.20 Å, and in Tl(OEP)Cl (OEP = octaethylporphyrin), 2.212 (6) Å.[12] Of relevance here is the Ct–N(pyrrole) distance of 2.104 (4) Å, which is to be compared with the 2.065 (7) Å found in (1-meim)MnTPP (meim = methylimidazole), 2.10 (1) Å for Tl(OEP)Cl, and 2.098 (8) Å for Cl_2SnTPP.[13] These distances are indicative of a substantially expanded porphyrin core. The porphyrin core is resistant to such expansion,[10] and this may contribute to the distortion of the porphyrin (vide infra). As expected, the Cd–N(axial) distance is longer at 2.323 (2) Å. The N–C(A) (α) distances are all within 3 standard deviations (0.005 Å) of the average, 1.368 Å). The C(A)–C(B) (α to β) distances are within 3 standard deviations (0.005 Å) of the average, 1.451 Å. The C(B)–C(B) (β to β) distances are within 2 standard deviations (0.005 Å) of the average, 1.357 Å. Figure 2 shows that the piperidine ring is in the expected chair conformation, similar to other metalloporphyrin piperidine adducts.[14] However, the Cd–N(5)–C(2P5) and Cd–N(5)–C(6P5) angles of 112.2 (2) and 113.6 (2)° respectively indicate that the nitrogen lone pair is directed toward the Cd atom. It is clear from Figure 2 and the pyrrole nitrogen–Cd–piperidine nitrogen angles that the piperidine is tilted off the Ct–Cd–N(5) axis toward the N(2)–N(3) bisector by about 10°.

Instead of the common "doming" or "tenting" found in analogous metalloporphyrins, a warping or hinge distortion is found. This warping may be described as the atoms, except for N(4) and N(1), on the N(4), N(1) side of the molecule being displaced away from the N(1), N(2), N(3), N(4) plane by varying amounts (see Figure 2 and Table V). This distortion, which is also reflected in the static ^{113}Cd NMR results, could come from three sources: from nonbonded intermolecular porphyrin–porphyrin interactions, from nonbonded intracomplex interactions between the piperidine ring and the porphyrin, or from the expansion of the porphyrin core by the relatively large metal atom. This last effect we tend to rule out because that should give rise to the previously observed "doming" or "tenting". The first possibility is most likely from an examination of nonbonded intermolecular interactions (Table IV) and the potential energy calculations (vide infra). With use of only intramolecular interactions, the energy is essentially independent of piperidine orientation (see also Figure 1). It is possible that the distortion may be a combination of intermolecular nonbonded interactions and core expansion effects. The message is clear that distortions in the porphyrin plane are just as likely to come from intermolecular packing effects as from electronic origins within the porphyrin. The remaining distances and angles are normal and are the expected values (see Table IV). There is no indication of a D_{2d} or ruffling distortion in this case. In addition, the Cd–N(pyrrole) distances are somewhat shorter than those observed for ordinary Cd–N chelate complexes at ~2.35 Å.[3] This result is not unexpected.

(9) Johnson, C. K. *Oak Ridge Natl. Lab., [Rep.] ORNL (U.S.)* **1973**, *ORNL-3794*.
(10) Scheidt, W. R. *Acc. Chem. Res.* **1977**, *10*, 339–345 and references therein.
(11) Rodesiler, P. F.; Griffith, E. A. H.; Amma, E. L.; Ellis, P. D. *J. Chem. Soc., Chem. Commun.* **1980**, 492–493.
(12) Cullen, D. L.; Meyer, E. F., Jr.; Smith, K. M. *Inorg. Chem.* **1977**, *16*, 1179–1186.
(13) Collins, D. M.; Scheidt, W. R.; Hoard, J. L. *J. Am. Chem. Soc.* **1972**, *94*, 6689–6696.
(14) Scheidt, W. R. *J. Am. Chem. Soc.* **1974**, *96*, 84–89.

Table IV. Interatomic Distances (Å) and Angles (deg) and Intermolecular Distances (Å) with Esd's in Parentheses

Distances

Cd(2+)–N(1)	2.190 (2)	C(1P1)–C(6P1)	1.404 (5)	C(3A)–C(3B)	1.456 (5)	C(3P4)–C(4P4)	1.357 (7)
Cd(2+)–N(2)	2.222 (2)	C(2P1)–C(3P1)	1.383 (6)	C(3A)–C(M2)	1.393 (5)	C(4P4)–C(5P4)	1.348 (7)
Cd(2+)–N(3)	2.209 (3)	C(3P1)–C(4P1)	1.397 (6)	C(3B)–C(4B)	1.357 (6)	C(5P4)–C(6P4)	1.409 (6)
Cd(2+)–N(4)	2.195 (2)	C(4P1)–C(5P1)	1.351 (6)	C(4A)–C(4B)	1.453 (5)	C(2P5)–C(3P5)	1.503 (6)
Cd(2+)–N(5)	2.323 (2)	C(5P1)–C(6P1)	1.412 (6)	C(4A)–C(M3)	1.417 (5)	C(3P5)–C(4P5)	1.496 (8)
N(1)–C(1A)	1.371 (4)	C(1P2)–C(2P2)	1.397 (5)	C(5A)–C(5B)	1.444 (5)	C(4P5)–C(5P5)	1.498 (8)
N(1)–C(2A)	1.378 (4)	C(1P2)–C(6P2)	1.399 (5)	C(5A)–C(M3)	1.410 (5)	C(5P5)–C(6P5)	1.501 (7)
N(2)–C(3A)	1.364 (5)	C(2P2)–C(3P2)	1.398 (6)	C(5B)–C(6B)	1.360 (5)	C(6)–C(1)	1.395 (6)
N(2)–C(4A)	1.365 (5)	C(3P2)–C(4P2)	1.374 (6)	C(6A)–C(6B)	1.453 (5)	C(6)–C(2)	1.395 (7)
N(3)–C(5A)	1.368 (5)	C(4P2)–C(5P2)	1.365 (6)	C(6A)–C(M4)	1.417 (5)	C(6)–C(7)	1.429 (8)
N(3)–C(6A)	1.360 (4)	C(5P2)–C(6P2)	1.403 (6)	C(7A)–C(7B)	1.449 (5)	C(1)–C(5)	1.396 (6)
N(4)–C(7A)	1.382 (4)	C(1P3)–C(2P3)	1.372 (5)	C(7A)–C(M4)	1.400 (5)	C(5)–C(4)	1.395 (7)
N(4)–C(8A)	1.360 (4)	C(1P3)–C(6P3)	1.382 (5)	C(7B)–C(8B)	1.358 (5)	C(4)–C(3)	1.395 (6)
N(5)–C(2P5)	1.481 (4)	C(2P3)–C(3P3)	1.380 (7)	C(8A)–C(8B)	1.449 (5)	C(3)–C(2)	1.394 (6)
N(5)–C(6P5)	1.467 (6)	C(3P3)–C(4P3)	1.382 (7)	C(8A)–C(M1)	1.407 (5)	C(2)–C(8)	1.455 (7)
C(1A)–C(1B)	1.455 (5)	C(4P3)–C(5P3)	1.339 (6)	C(M1)–C(1P1)	1.506 (5)	Ct–N(1)	2.091 (5)
C(1A)–C(M1)	1.412 (5)	C(5P3)–C(6P3)	1.407 (6)	C(M2)–C(1P2)	1.504 (5)	Ct–N(2)	2.113 (5)
C(1B)–C(2B)	1.354 (5)	C(1P4)–C(2P4)	1.374 (5)	C(M3)–C(1P3)	1.509 (5)	Ct–N(3)	2.102 (5)
C(2A)–C(2B)	1.447 (5)	C(1P4)–C(6P4)	1.382 (5)	C(M4)–C(1P4)	1.510 (5)	Ct–N(4)	2.108 (5)
C(2A)–C(M2)	1.419 (5)	C(2P4)–C(3P4)	1.397 (7)	C(1P1)–C(2P1)	1.393 (5)	Ct–Cd	0.657 (3)

Angles

N(1)–Cd(2+)–N(2)	85.0 (1)	C(1A)–C(M1)–C(1P1)	116.7 (3)	N(1)–C(2A)–C(2B)	108.2 (3)	C(2P3)–C(1P3)–C(6P3)	121.3 (4)
N(1)–Cd(2+)–N(3)	144.8 (1)	C(8A)–C(M1)–C(1P1)	116.4 (3)	N(1)–C(2A)–C(M2)	126.1 (3)	C(1P3)–C(2P3)–C(3P3)	118.7 (4)
N(1)–Cd(2+)–N(4)	84.8 (1)	C(2A)–C(M2)–C(3A)	127.0 (3)	C(2B)–C(2A)–C(M2)	125.7 (3)	C(2P3)–C(3P3)–C(4P3)	121.8 (5)
N(1)–Cd(2+)–N(5)	114.1 (1)	C(2A)–C(M2)–C(1P2)	115.9 (3)	C(1B)–C(2B)–C(2A)	107.8 (3)	C(3P3)–C(4P3)–C(5P3)	118.2 (4)
N(2)–Cd(2+)–N(3)	84.7 (1)	C(3A)–C(M2)–C(1P2)	116.9 (3)	N(2)–C(3A)–C(3B)	107.7 (3)	C(4P3)–C(5P3)–C(6P3)	122.7 (4)
N(2)–Cd(2+)–N(4)	145.9 (1)	C(4A)–C(M3)–C(5A)	127.2 (3)	N(2)–C(3A)–C(M2)	126.2 (3)	C(1P3)–C(6P3)–C(5P3)	117.3 (4)
N(2)–Cd(2+)–N(5)	101.8 (1)	C(4A)–C(M3)–C(1P3)	115.7 (3)	C(3B)–C(3A)–C(M2)	126.1 (3)	C(M4)–C(1P4)–C(2P4)	119.4 (3)
N(3)–Cd(2+)–N(4)	85.1 (1)	C(5A)–C(M3)–C(1P3)	117.1 (3)	C(3A)–C(3B)–C(4B)	107.8 (3)	C(M4)–C(1P4)–C(6P4)	119.3 (3)
N(3)–Cd(2+)–N(5)	101.0 (1)	C(6A)–C(M4)–C(7A)	126.7 (3)	N(2)–C(4A)–C(4B)	108.5 (3)	C(2P4)–C(1P4)–C(6P4)	121.3 (3)
N(4)–Cd(2+)–N(5)	112.1 (1)	C(6A)–C(M4)–C(1P4)	116.0 (3)	N(2)–C(4A)–C(M3)	125.6 (3)	C(1P4)–C(2P4)–C(3P4)	118.5 (4)
Cd(2+)–N(1)–C(1A)	126.1 (2)	C(7A)–C(M4)–C(1P4)	117.2 (3)	C(4B)–C(4A)–C(M3)	125.9 (3)	C(2P4)–C(3P4)–C(4P4)	121.7 (4)
Cd(2+)–N(1)–C(2A)	125.0 (2)	C(M1)–C(1P1)–C(2P1)	120.8 (3)	C(3B)–C(4B)–C(4A)	106.8 (3)	C(3P4)–C(4P4)–C(5P4)	119.0 (4)
C(1A)–N(1)–C(2A)	108.3 (3)	C(M1)–C(1P1)–C(6P1)	118.6 (3)	N(3)–C(5A)–C(5B)	108.0 (3)	C(4P4)–C(5P4)–C(6P4)	122.2 (4)
Cd(2+)–N(2)–C(3A)	124.1 (2)	C(2P1)–C(1P1)–C(6P1)	120.6 (3)	N(3)–C(5A)–C(M3)	126.2 (3)	C(1P4)–C(6P4)–C(5P4)	117.4 (4)
Cd(2+)–N(2)–C(4A)	123.8 (2)	C(1P1)–C(2P1)–C(3P1)	119.4 (4)	C(5B)–C(5A)–C(M3)	125.8 (3)	N(5)–C(2P5)–C(3P5)	113.2 (3)
C(3A)–N(2)–C(4A)	109.2 (3)	C(2P1)–C(3P1)–C(4P1)	121.0 (4)	C(5A)–C(5B)–C(6B)	107.6 (3)	C(2P5)–C(3P5)–C(4P5)	111.7 (4)
Cd(2+)–N(3)–C(5A)	123.6 (2)	C(3P1)–C(4P1)–C(5P1)	119.0 (4)	N(3)–C(6A)–C(6B)	108.2 (3)	C(3P5)–C(4P5)–C(5P5)	110.8 (4)
Cd(2+)–N(3)–C(6A)	124.3 (2)	C(4P1)–C(5P1)–C(6P1)	122.5 (4)	N(3)–C(6A)–C(M4)	126.4 (3)	C(4P5)–C(5P5)–C(6P5)	111.4 (4)
C(5A)–N(3)–C(6A)	109.2 (3)	C(1P1)–C(6P1)–C(5P1)	117.5 (3)	C(6B)–C(6A)–C(M4)	125.4 (3)	N(5)–C(6P5)–C(5P5)	114.2 (4)
Cd(2+)–N(4)–C(7A)	125.3 (2)	C(M2)–C(1P2)–C(2P2)	120.7 (3)	C(5B)–C(6B)–C(6A)	107.0 (3)	C(1)–C(6)–C(2)	120.0 (4)
Cd(2+)–N(4)–C(8A)	126.5 (2)	C(M2)–C(1P2)–C(6P2)	118.8 (3)	N(4)–C(7A)–C(7B)	108.6 (3)	C(1)–C(6)–C(7)	120.2 (5)
C(7A)–N(4)–C(8A)	107.8 (3)	C(2P2)–C(1P2)–C(6P2)	120.6 (3)	N(4)–C(7A)–C(M4)	126.1 (3)	C(2)–C(6)–C(7)	119.7 (5)
Cd(2+)–N(5)–C(2P5)	112.2 (2)	C(1P2)–C(2P2)–C(3P2)	118.6 (4)	C(7B)–C(7A)–C(M4)	125.1 (3)	C(6)–C(1)–C(5)	119.9 (4)
Cd(2+)–N(5)–C(6P5)	113.6 (2)	C(2P2)–C(3P2)–C(4P2)	121.5 (4)	C(7A)–C(7B)–C(8B)	107.1 (3)	C(1)–C(5)–C(4)	120.0 (4)
C(2P5)–N(5)–C(6P5)	109.6 (3)	C(3P2)–C(4P2)–C(5P2)	119.3 (4)	N(4)–C(8A)–C(8B)	109.2 (3)	C(5)–C(4)–C(3)	120.0 (4)
N(1)–C(1A)–C(1B)	108.4 (3)	C(4P2)–C(5P2)–C(6P2)	121.8 (4)	N(4)–C(8A)–C(M1)	125.6 (3)	C(4)–C(3)–C(2)	120.0 (4)
N(1)–C(1A)–C(M1)	125.8 (3)	C(1P2)–C(6P2)–C(5P2)	118.2 (4)	C(8B)–C(8A)–C(M1)	125.0 (3)	C(6)–C(2)–C(3)	120.0 (4)
C(1B)–C(1A)–C(M1)	125.8 (3)	C(M3)–C(1P3)–C(2P3)	119.1 (3)	C(7B)–C(8B)–C(8A)	107.3 (3)	C(6)–C(2)–C(8)	121.9 (4)
C(1A)–C(1B)–C(2B)	107.3 (3)	C(M3)–C(1P3)–C(6P3)	119.6 (3)	C(1A)–C(M1)–C(8A)	126.8 (3)	C(3)–C(2)–C(8)	118.0 (4)

Intermolecular Distances Less Than 3.85 Å Involving the Porphyrin Core

atom	symmetry transformation[a]	atom	dist
C(1A)	(16)	C(3P2)	3.718 (7)
	(16)	C(2P2)	3.677 (8)
C(1B)	(16)	C(2P2)	3.771 (7)
C(4B)	(16)	C(6P3)	3.748 (6)
	(16)	C(4P4)	3.775 (7)
C(5B)	(16)	C(3P4)	3.718 (7)
C(6B)	(16)	C(3P1)	3.666 (8)
	(16)	C(2P4)	3.707 (8)
	(16)	C(3P4)	3.731 (7)
C(7B)	(16)	C(5P1)	3.735 (7)
C(8B)	(15)	C(4P2)	3.812 (7)
	(16)	C(5P1)	3.832 (8)
	(16)	C(6P1)	3.638 (7)

[a] Symmetry transformations: (15) $+x, -y, -z$; (16) $-1 + x, y, z$.

The immediate, most striking aspect of the solution ^{113}Cd NMR (see Table II) is its relative insensitivity to the nature of the axial nitrogen donor ligands in the CdTPP·L five-coordinate complexes, 418–438 ppm. Even the very weak oxygen donor tetrahydrofuran at +434 ppm falls into this range, and only an extreme change in ligand, such as triphenylphosphine, gives a ^{113}Cd chemical shift of 498 ppm. Therefore, the features of the ^{113}Cd nMR spectra of CdTPP·L and other five-coordinate CdTPP type complexes are dominated by the porphyrin ring system, a not surprising result. Hence, any ^{113}Cd NMR experiments that wish to use this nucleus

Table V. Deviations (Å) for Least-Squares Planes

Plane Defined by N(1), N(2), N(3), N(4)

Equation of the Form $PX + QY + RZ = S$, Where $P = 0.0307$, $Q = 0.8967$, $R = -0.4415$, $S = 2.1024$

atom	dev	atom	dev	atom	dev	atom	dev
Cd	−0.657	C(1B)	0.406	C(5A)	0.002	C(8B)	0.422
N(1)	0.009	C(2A)	0.133	C(5B)	0.056	C(M1)	0.220
N(2)	−0.009	C(2B)	0.368	C(6A)	0.076	C(M2)	0.096
N(3)	0.009	C(3A)	0.036	C(6B)	0.109	C(M3)	−0.011
N(4)	−0.009	C(3B)	0.048	C(7A)	0.142	C(M4)	0.146
N(5)	−2.956	C(4A)	−0.011	C(7B)	0.395	Ct	−0.000
C(1A)	0.190	C(4B)	0.017	C(8A)	0.170		

Plane Defined by N(1)···C(M4)

Equation of the Form $PX + QY + RZ = S$, Where $P = 0.0041$, $Q = 0.9161$, $R = -0.4009$, $S = 2.1646$

atom	dev	atom	dev	atom	dev	atom	dev
Cd	−0.660	C(1B)	0.233	C(5B)	0.224	C(M1)	0.036
N(1)	−0.066	C(2A)	0.007	C(6A)	0.126	C(M2)	0.108
N(2)	0.073	C(2B)	0.249	C(6B)	0.223	C(M3)	0.166
N(3)	0.076	C(3A)	0.111	C(7A)	0.060	C(M4)	0.127
N(4)	−0.096	C(3B)	0.193	C(7B)	0.244	Ct	−0.004
N(5)	−2.939	C(4A)	0.139	C(8A)	0.014		
C(1A)	0.0045	C(4B)	0.141	C(8B)	0.225		

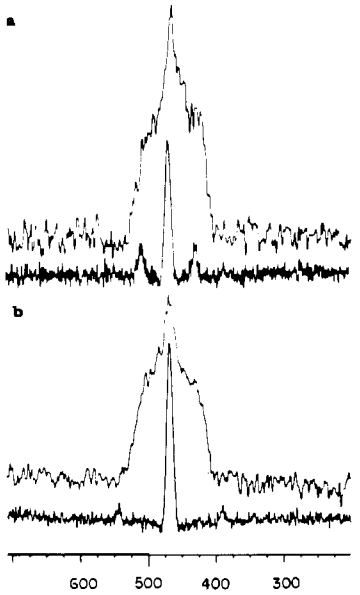

Figure 3. The ^{113}Cd NMR natural-abundance powder spectra of (a) the *o*-xylene solvate of the piperidine adduct of (5,10,15,20-tetraphenylporphyrinato)cadmium(II) and b the unsolvated piperidine adduct of (a). The MAS results are indicated below each of parts a and b. To all intents and purposes the spectra of parts a and b are identical.

as a probe via the chemical shift of the differences at the metal site in heme groups upon the R ⇌ T allosteric transformation will have, at best, limited success.

Another feature of the solution ^{113}Cd NMR spectra of these CdTPP·L compounds is that with the substituted pyridines there is a regular trend in which the stronger the donor the substituted pyridine becomes, the more shielded the Cd nucleus becomes. However, the total observed range is small, 418–432 ppm. This is in the direction opposite to that which one would have predicted. However, there chemical shifts are due to the interplay of various factors and caution should be exercised in their interpretation. One such factor is that we may be observing the average of more than one species in solution.

In the static powder spectrum of (tetraphenylporphyrinato)-cadmium(II)–piperidine it is to be noted (Figure 3) that with the *o*-xylene molecule of crystallization there are clearly three components to the chemical shielding tensor, with chemical shift values at 522, 470, and 412 ppm. Without the *o*-xylene of crystallization,

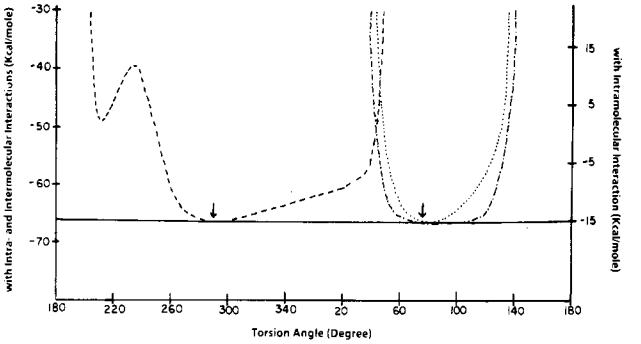

Figure 4. Potential energy (kcal/mol) calculated as function of torsion angles (deg): N(1)--Cd(1)--N(5)--C(2P5) intra- and intermolecular interactions (---); C(1A)--C(1M)--C(1P1)--C(1P2) (only for 0–180° range) intramolecular interactions only (-·-·-); intra- and intermolecular interactions (···). Arrows show the values observed in the crystal structure and correspond well to the minima.

these values are essentially unchanged at 528, 468, and 414 ppm, respectively. The high and low extremes are ±50 ppm from the center value, which is the same as the MAS result. However, this value is considerably different from the chloroform solution value of 438 ppm (see Table IV). This reflects a relaxation of intermolecular distortions. The relatively high value of the chemical shift of unliganded Cd(TTP) at +476 ppm can be most readily interpreted as the formation of insoluble polymers. At higher temperatures sufficient dimer is formed that we are observing the ^{113}Cd NMR spectrum of the dimer. The dimer would be such that a pyrrole nitrogen of one porphyrin provides the fifth coordination site for the Cd of the other half of the dimer. Cd would be displaced from the "plane" of its four pyrrole nitrogens toward the other half of the dimer. However, the Cd–N distance would be relatively long in order to accommodate the nonbonded repulsions between porphyrins. Polymers for metalloporphyrins in solution are well-known. Again, it must be recognized that we may be looking at the average of more than one solution species. The above argument is the simplest but not necessarily a unique description.

It is of interest to compare structure results of the present piperidine adduct with that of an analogous pyridine adduct. The static ^{113}Cd NMR solid-state results of the pyridine adduct of cadmium tetraphenylporphyrin[4] appear to show C_4 axial symmetry. The crystal structure, except for two molecules in the asymmetric unit, shows the pyridine adduct to be very similar to the present structure.[15] There is no evidence in the present structure for abnormally large thermal motions of the piperidine molecule, nor is there in the pyridine structure, albeit the diffraction data in that case are limited and are of poorer quality. Therefore, an interpretation in the pyridine adduct and the present compound of rapid motions between alternative sites for the ligand seems unlikely. In this context we have carried out potential energy calculations for the present piperidine structure using the program EENY.[16] Atom–atom potential parameters were those of Pavel, Quagliata,, and Scarcelli.[17] The positions of the hydrogen atoms were calculated on the basis of the geometry of the heavy atoms, and for methylene groups the extended atom potentials were used. The piperidine molecule was rotated about the Cd–N(5) bond and the crystal lattice potential energy calculated as a function of the N(1)–Cd–N(5)–C(2P5) torsion angle. A broad minimum was observed corresponding to the observed angle of 68.7 (1)° (see Figure 4). A steep barrier of >30 Kcal/mol was observed between 50 and 200 °C. Thus, in this case rotation, or potential well hopping, is not possible in the crystal without large deformation of the Cd^{2+} coordination geometry. This is in marked contrast to the pyridine case, where a similar

(15) Lebioda, L., unpublished results.
(16) Motherwell, W. D. S. "EENY", Potential Energy Program; University of Cambridge: Cambridge, England; 1974.
(17) Pavel, N. V.; Quagliata, C.; Scarcelli, N. *Z. Kristallogr.* **1976**, *144*, 64–75.

calculation indicated virtually no barrier.[13] Thus, in the present piperidine case the structure, static solid-state ^{113}Cd NMR, and potential energy calculations are in complete agreement.

Acknowledgment. We wish to thank the PHS for research support via Grant No. GM-27721 and the NSF-supported regional NMR centers at the University of South Carolina (Grant No. CHE 78-18723) and Colorado State University (Grant No. CHE 78-18581) for their help, discussions, and assistance with the ^{113}Cd NMR data. We are also grateful to Paul Majors for the static powder spectra and discussions concerning their interpretation.

Supplementary Material Available: Listings of H atom positions, anisotropic thermal parameters, and observed and calculated structure amplitudes (51 pages). Ordering information is given on any current masthead page.

Contribution from the Department of Chemistry,
Faculty of Science, Osaka University, Toyonaka, Osaka 560, Japan

Kinetic Optical Resolution of Metal Complexes through a Stereoselective Adsorption and Inhibition Mechanism Caused by Chiral Additives

Kazuaki Yamanari* and Yoichi Shimura

Received March 1, 1985

Four kinds of conglomerates, ΔΛ-$[Co(aet)(en)_2](ClO_4)_2$, ΔΛ-$[Co(ox)(en)_2]Cl\cdot 4H_2O$, ΔΛ-$[Co(ox)(en)_2]Br\cdot H_2O$, and ΔΛ-$[Co(NO_2)_2(en)_2]Cl$ (aet = 2-aminoethanethiolate(1−), ox = oxalate(2−), and en = ethylenediamine), were kinetically resolved by crystallization in the presence of chiral additives Δ′- (or Λ′-) $[Co(AB)(en)_2]X_n$ (AB = two unidentate ligands or one bidentate ligand). The resolution mechanism is best explained in terms of stereoselective adsorption of the chiral additive at the crystal surfaces of one enantiomer of the same absolute configuration as the chiral additive and a drastic decrease of the growth rate of these crystals, as proposed by Addadi et al. Three characteristic aspects of this mechanism, i.e. preferential crystallization of the opposite enantiomer, stereoselective adsorption of the chiral additive, and a morphological change in the crystals of one enantiomer having the same absolute configuration as the chiral additive, were all observed in the present systems. Detailed study of the system ΔΛ-$[Co(ox)(en)_2]Cl$ (substrate)−Λ′-$[Co(gly)(en)_2]Cl_2$ (chiral additive; gly = glycinate(1−)) revealed that this kind of resolution takes place repeatedly, with alternative crystallization of Δ- and Λ-$[Co(ox)(en)_2]Cl\cdot 4H_2O$. The relationship between the enantiomeric excess and the crystal yield of the partially resolved substrate and the role of the chiral additive are discussed on the basis of the measurement of the solubilities in the supernatant solution. The above kinetic resolution was also found to be applicable to some substrates of racemic compound.

Introduction

Many resolution methods for metal complexes are known, such as diastereomer formation and column chromatography. Most of these methods are based on the electrostatic attraction between the complex ion and the oppositely charged ion of the resolving agent. However, as a special method of optical resolution, it has been reported that a certain chiral additive, which has the same kind of charge as the substrate,[1] can behave as an efficient resolving agent. For example, Werner reported the resolution of ΔΛ-$[Co(NO_2)_2(en)_2]Cl$ using Λ-$[Co(ox)(en)_2]Cl$ as a chiral additive.[2] Broomhead resolved ΔΛ-$[Co(ox)(en)_2]CH_3CO_2$ with a mixture of Λ-$[Co(en)_3](CH_3CO_2)_3$ + KBr to give a 40% yield of Δ-$[Co(ox)(en)_2]Br$.[3] It has been suggested that hydrogen bonding[3] and configurational activity[4] are responsible for these phenomena, but no mechanistic investigation has been performed thus far.

We were interested in the recent investigations by Addadi et al., who reported the optical resolution of organic conglomerates with the assistance of "tailor-made impurities".[5] The mechanism is based on stereoselective adsorption of a chiral additive and inhibition of crystal growth, as shown in Figure 1. In the absence of a Λ′-chiral additive that is stereochemically similar to one enantiomer (Λ) of the conglomerate substrate, the two crystallization rates k_Δ and k_Λ are equal.[6] In the presence of a Λ′-chiral additive, however, it is adsorbed on the Λ-crystals and inhibits their crystal growth, leading to $k_\Delta > k_\Lambda$. Therefore, the enantiomer crystallized in excess first has the absolute configuration opposite to that of the chiral additive ("rule of reversal"), and the affected enantiomer, Λ, should be found in the second crop of crystals. This mechanism can account for the experimental results of Werner and Broomhead.[7]

We report here a systematic investigation of a kinetic resolution of metal complexes due to chiral additives. Both the substrates and the chiral additives used in this paper belong to the same complex type of $[Co(AB)(en)_2]X_n$ (AB = two unidentate ligands or one bidentate ligand). Several combinations of the substrates and the chiral additives were found to show high resolution percentages. A detailed study in the system ΔΛ-$[Co(ox)(en)_2]$-Cl−Λ′-$[Co(gly)(en)_2]Cl_2$ (CA)[8] revealed that the resolution process occurs time after time and apparent supersaturation of the Λ-substrate increases with concentration of the chiral additive. It was found that this resolution is applicable not only to conglomerates but also to some racemic compounds.

Experimental Section

Preparation of Metal Complexes. The following cobalt(III) complexes used in this study were prepared and/or resolved according to methods described in the literature and were converted into the desired salts by using QAE-Sephadex A-25: ΔΛ-, Δ-, and Λ-$[Co(aet)(en)_2](ClO_4)_2$:[9]

(1) The terminology of chiral substances is based on that given in: Jacques, J.; Collet, A.; Wilen, S. H. "Enantiomers, Racemates and Resolutions"; Wiley: New York, 1981. *Substrate* denotes the racemic complex to be optically resolved. *Racemate* is an equimolar mixture of two enantiomers whose physical state is unspecified or unknown. *Conglomerate* (or *Racemic mixture*) is a mechanical mixture of crystals of the two pure enantiomers and is formed as a result of a spontaneous resolution. *Racemic compound* is a homogeneous solid in which two enantiomers are present in equal quantities in a well-defined arrangement within the crystal lattice.
(2) Werner, A. *Chem. Ber.* **1914**, *47*, 2171.
(3) Broomhead, J. A. *Nature (London)*, **1966**, *211*, 742.
(4) Dwyer, F. P.; Gyarfas, E. C.; Dwyer, M. F. O. *Nature (London)*, **1951**, *167*, 1036.
(5) Addadi, L.; van Mil, J.; Lahav, M. *J. Am. Chem. Soc.* **1981**, *103*, 1249. Addadi, L.; Weinstein, S.; Gati, E.; Weissbuch, I.; Lahav, M. *J. Am. Chem. Soc.* **1982**, *104*, 4610.
(6) Greek letters Δ (or Λ) and Δ′ (or Λ′) represent the absolute configurations of substrates and chiral additives, respectively.
(7) Werner reported that Λ-$[Co(NO_2)_2(en)_2]Cl$ is deposited by the addition of Λ′-$[Co(ox)(en)_2]Cl$,[1] but the opposite Δ-configuration was confirmed to appear as the first crystals by our reinvestigation.
(8) CA denotes a chiral additive.
(9) (a) Nosco, D. L.; Deutsch, E. *Inorg. Synth.* **1982**, *21*, 19. (b) Yamanari, K.; Hidaka, J.; Shimura, Y. *Bull Chem. Soc. Jpn.* **1977**, *50*, 2299. (c) Yamanari, K.; Shimura, Y. *Bull. Chem. Soc. Jpn.* **1983**, *56*, 2283.

0020-1669/85/1324-4600$01.50/0